Rain-induced bistatic scattering at 60 GHz

Rain-induced Bistatic Scattering at 60 GHz

Robert J Watson[#1], Henry T van der Zanden[*2], Matti H A J Herben[#3]

[#1]*Dept. Electronic & Electrical Engineering, University of Bath, Bath, UK*

[1]r.j.watson@bath.ac.uk

[*2]*Philips Research Eindhoven (formerly with Eindhoven University of Technology (TU/e)), Eindhoven, NL*

[2]henryvanderzanden@gmail.com

[#3]*Eindhoven University of Technology (TU/e), Eindhoven, NL*

[3]m.h.a.j.herben@tue.nl

***Abstract*—The 60 GHz oxygen absorption band has been of particular interest in recent years for short-hop links between buildings in dense urban environments. The high oxygen attenuation in this band, typically in the range 12-16 dB km^{-1}, limits its practical use for longer links and for Earth-space communications. However, the high attenuation results in very short frequency-reuse distances making these systems extremely well suited for high link-density deployments. However when rain falls on a link it may act as a coupling mechanism causing interference on adjacent line-of-sight links. In this paper we study the effects of rain-induced bistatic scattering on 60 GHz links and its potential impact on link planning and assignment.**

I. INTRODUCTION

Recently there has been considerable interest in the 60 GHz frequency band for short-distance fixed point-to-point links including so-called "last-mile" communications. Typical link lengths are < 2.5 km. The high oxygen attenuation in this band (typically 12-16 dB km^{-1}) limits its practical use for longer terrestrial links and also for Earth-space communication. The main application therefore is for indoor networking or outdoors in dense urban environments where a high density of short links might be expected. A typically deployed commercial radio system is the Nokia Metrohopper which has a 1.5° half-power beamwidth.

For point-to-point links, one of the key advantages of the 60 GHz band is the relatively high directivity achievable from a physically small antenna. The narrow beam-widths and low side-lobe levels achievable mean that the signal power outside the narrow main lobe is very low. This effect is compounded by the high oxygen attenuation in the 60 GHz frequency band, which results in an even faster decrease of signal power outside the main beam. At 60 GHz the oxygen attenuation typically results in very short frequency-reuse distances making these systems extremely well suited for high-link density deployments with minimum interference between the links. However, when rain falls on the link, there is the potential for interference due to bistatic coupling between nearby links.

Hydrometeor scatter, usually dominated by rain, has been extensively modelled as an anomalous propagation mechanism leading to coupling between terrestrial point-to-point links and Earth-space links, e.g., [1]. Much of the early work on hydrometeor scatter stemmed from work on rain-induced signal enhancement on tropospheric scatter links at frequencies below 30 GHz. Some of the first modelling attempts, backed-up with experimental measurements, are those of [2]. These experiments considered relatively long paths (~140 km) at low microwave frequencies (4-8 GHz). As part of the European COST 210 project in the mid-1980s a considerable volume of experimental data was collected on rain-scatter. Again however, the focus of the study was for the determination of terrestrial-link to Earth-station interference at frequencies below 30 GHz.

The wavelength, the size and number density of the scatterers determines the approach to the modelling of bistatic scattering, whether single-scattering or multiple-scattering. In the single-scattering regime it is assumed that the incident wave reaches the scatterer (raindrop) after weakly interacting with only relatively few other scatterers (Fig. 1(a)). For each scatterer the incident wave is considered to be the direct wave from the source. Incident waves from interactions with other scatterers are considered negligible. As the number density of scatterers increases or the strength of scattering increases (as may occur with increasing frequency) multiple scattering may become important (Fig 1(c)).

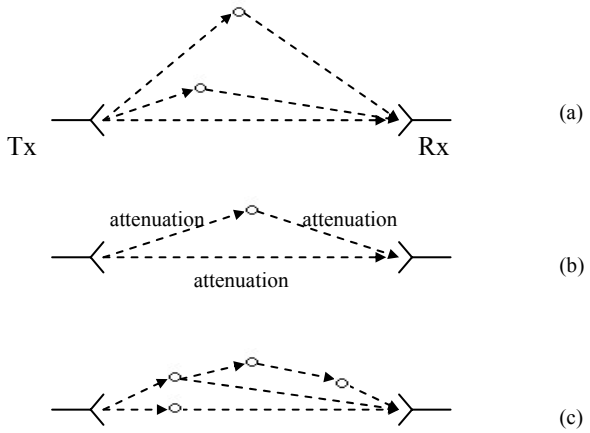

Figure 1: Scattering approximations (after [1]); (a) Single scattering, (b) first-order multiple scattering, (c) multiple-scattering.

Previous work by [3, 4] suggests that these effects may be considered negligible below 100 GHz with narrow beam antennas. This was experimentally tested at 94 GHz by [5] who found the first-order multiple scattering approach, where

only the attenuation to the scattering volume along the path is considered, is a sufficient (Fig 1(b)).

II. Modelling Bistatic Coupling

Following the approach of [5], in this study at 60 GHz we consider the first-order multiple-scattering approach to be valid. The relationship between the physical processes responsible for this scattering and the coupling it produces can therefore be described by the bistatic radar equation (1). Evaluation of this equation permits the determination of the coupling between two antenna beams having a scatterer filled common volume, V_c. The power scattered from one antenna beam into the other, P_r, can be written as;

$$P_r = \frac{P_t \lambda^2 A_1 A_2}{(4\pi)^3 R_1^2 R_2^2} \iiint_{V_c} G_1 G_2 a_1 a_2 \eta_s dV \qquad [1]$$

where: P_t is the transmitted power, λ is the wavelength, R_1, R_2 are the distances between each of the antennas and the common (scattering) volume, A_1, A_2 are the path attenuations to the scattering volume (which at ~ 60 GHz will have a persistent dominant contribution due to atmospheric oxygen absorption), G_1, G_2 are the antenna gain functions, a_1, a_2 are attenuations within the common volume and η_s is the bistatic reflectivity function. The bistatic reflectivity function is dependent on the scattering properties of the particles (assumed in this study to be only raindrops) and also on the particle size distribution. This approach is a first-order multiple-scattering approach i.e. the transmitted wave propagates through the rain medium, is scattered by an elemental volume and propagates through the rain medium along the path to the receiver. The bistatic reflectivity function η_s can be written in terms of the raindrop size distribution function (DSD), $n(\bar{a})d(\bar{a})$, as;

$$\eta_s = C \int_0^\infty n(\bar{a}) \sigma_s(\bar{a}) d\bar{a}, \qquad [2]$$

where: σ_s is the bistatic scattering cross-section which is a function of the size of the scatterer and scattering geometry and C is a constant involving the refractive index of the drop (itself a function of temperature). Calculation of the bistatic scattering cross-section in rain can be performed using simple Mie theory (assuming raindrops can be modelled as spheres) or using a method such as the Fredholm integral method (which allows scatterers to be modelled as spheroids). In this study we opted to use simple Mie theory as the uncertainty in the raindrop size distribution is likely to far outweigh the differences in scattering between sphere and spheroid assumptions for raindrop shape. Finally, integration of the bistatic radar equation can be solved using numerical integration techniques e.g., Romberg's method [6, 7].

Under certain conditions it is possible to simplify the analysis through a number of assumptions. If narrow beam-width antennas are used such that the beam patterns can be modelled as constant gain cones, it is then possible to determine an analytic solution for the common volume between the two overlapping beams [1];

$$V_c = \frac{\pi\sqrt{\pi}}{8(\ln 2)^{3/2}} \frac{R_1^2 R_2^2 \theta_1 \theta_2 \phi_1 \phi_2}{\left[R_1^2 \phi_1^2 + R_2^2 \phi_2^2\right]^{1/2}} \frac{1}{\sin\theta_s}, \qquad [3]$$

where θ_1 and Φ_1 are the half-power beamwidths of the transmitter, θ_2 and Φ_2 are the half-power beamwidths of the receiver and θ_s is the scattering angle. This assumption is most likely valid for point-to-point links where antenna half-power beam-widths are around 0.5-3° and the sidelobes are at least 20 dB down from the main lobe (e.g., for compliancy with ETSI EN300 833 antenna pattern masks).

Furthermore it may also be possible to assume that the bistatic scattering function (2) also remains constant throughout the scattering volume. These assumptions greatly simplify the solution as they effectively decouple the scattering and volume integrals, reducing the solution of (1) to a simple product [2, 8].

III. Bistatic Scattering

A. *Bistatic scattering from individual raindrops*

Assuming that raindrops can be approximated as isotropic homogeneous spheres, Mie theory can be used to describe the scattering properties of raindrops. At the frequencies considered here the wavelength and the raindrop diameter are of similar order hence we are clearly in the Mie scattering regime [9]. Figure 2 shows the forward and backward scattering efficiencies as a function of drop radius from 0 to 4 mm.

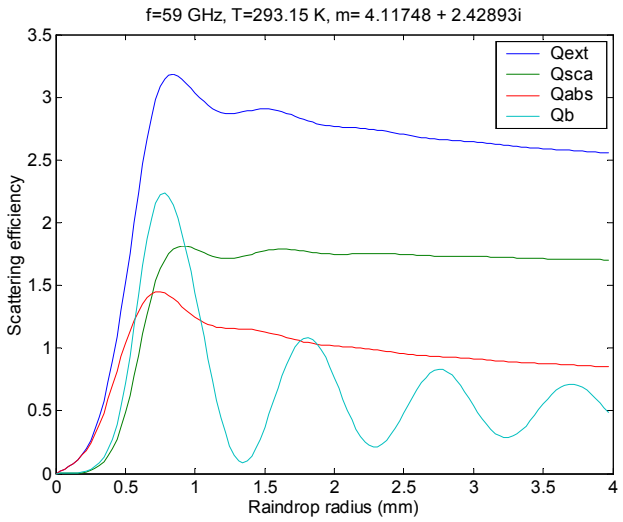

Figure 2: Mie scattering efficiencies at 59 GHz at a temperature of 20°C.

Scattering efficiency is defined as the scattering cross-section normalised to the drop's geometric cross-section;

$$\sigma_{ext} = Q_{ext}(\pi a)^2, \quad Q_{ext} = Q_{sca} + Q_{abs} \qquad [4]$$

Four curves are shown in Fig. 2: Q_{ext} the extinction efficiency, the Q_{sca} the scattering efficiency, Q_{abs} the absorption efficiency and Q_b the back-scattering (or radar) efficiency. Similar behaviour is seen between 59 GHz and 66 GHz. The wavenumber, k_0, changes only fractionally across the band: 1.24×10^{-3} m^{-1} at 59 GHz to 1.38×10^{-3} m^{-1} at 66 GHz.

The importance of small drops at high frequencies is often cited in the literature. From Fig. 2 it can be seen that drops upto around 0.75 mm are in the Rayleigh scattering regime. Larger sizes are clearly in the Mie regime. For drops >0.5 mm radius the scattering and absorption efficiencies are significant and relatively constant indicating that there is likely to be strong forward scatter and absorption across all raindrop sizes.

B. Scattering from populations of raindrops

In order to consider scattering from rain we must consider a population of raindrops. This necessitates information on the raindrop size distribution. The most commonly used DSD is the Marshall-Palmer DSD which can be written in terms of the equivalent volume drop radius $\bar{a}$ as;

$$n(\bar{a}) = N_0 \exp(-\Lambda \bar{a}), \qquad [5]$$

where $N_0 = 1.6 \times 10^4$ m^{-3} mm^{-1} the slope parameter $\Lambda = 8.2 R^{-0.21}$, R is the rainfall rate in mm h^{-1}.

The integrand of (2) calculated using the Marshall-Palmer DSD for the various scattering functions as a function of drop radius is shown in Figs. 3 and 4.

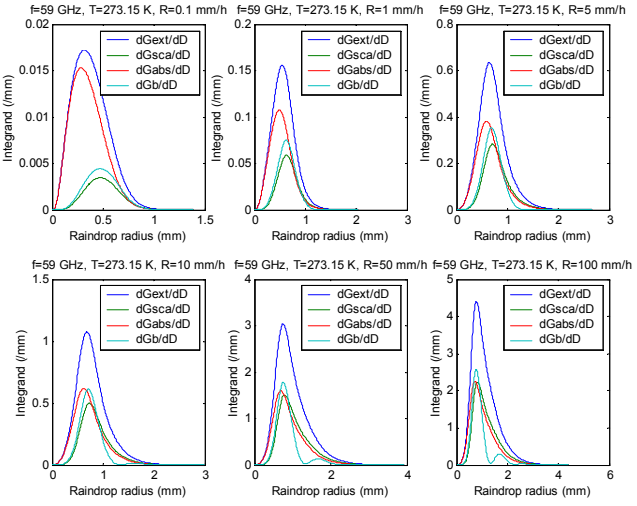

Figure 3: Integrand of equation 2 (scattering function weighted by DSD) as a function of rainfall rate from 0.1 - 100 mm h^{-1} at 0°C, for a Marshall-Palmer DSD at 59 GHz.

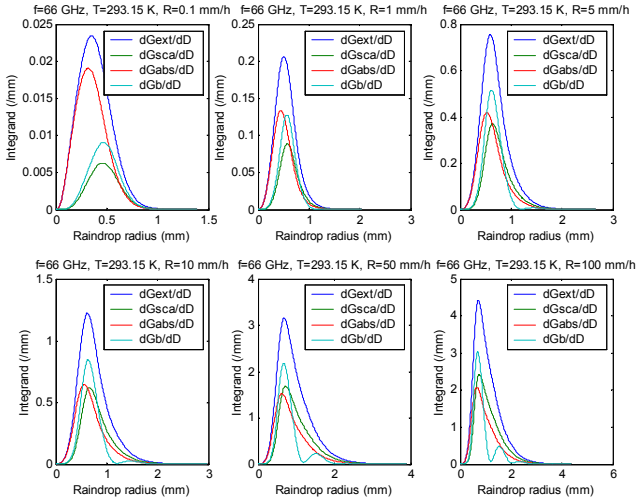

Figure 4: Integrand of equation 2 (scattering function weighted by DSD) as a function of rainfall rate from 0.1 - 100 mm h^{-1} at 20°C, for a Marshall-Palmer DSD at 66 GHz.

In spite of their smaller scattering amplitudes, it can be seen that for rainfall rates most often observed in temperate climates, small raindrops of 0.5-1.5 mm radius are the most significant. As an aside, note that as if often the case at other frequencies, the size weighting of forward scattering is different from backward scattering. It is for this reason that it is often difficult to find dropsize distribution independent relationships between forward and backward scattering processes (e.g., radar reflectivity and attenuation).

C. Scattering as a function of bistatic angle

Thus far we have only considered only forward and backward scattering (scattering angles of 0° and 180° respectively). In real-world link assignments many link geometries (and therefore many scattering angles) must be considered.

Using Mie theory is possible to calculate the angular scattering pattern [9]. To avoid confusion with forward and backward scattering we refer to this as the scattering intensity (differential scattering cross-section). Figures 4 through 9 show normalized scattered intensity polar plots for horizontal (shown in blue) and vertical (shown in red) incident polarizations. The sum of the two intensities is also shown (coloured cyan). In all figures the frequency is 59 GHz and the temperature is 20°C. Similar behaviour is seen at 66 GHz, and at 0°C.

It can be seen that the smaller drop sizes, up to around 0.5 mm in radius (Figs. 5 and 6), show dipole-like scattering patterns as one might intuitively expect from drops almost in the Rayleigh scattering regime. Scattering in the forward scattering is slightly greater than in the backward direction. For larger drop sizes shown in Figs. 7, 8 scattering becomes progressively dominated by forward scattering. Less difference can also be seen between horizontal and vertical

incident polarisations. For the very largest drops generally observed, forward scattering is dominant. Almost no difference between horizontal and vertical polarisations can be seen (Fig. 9).

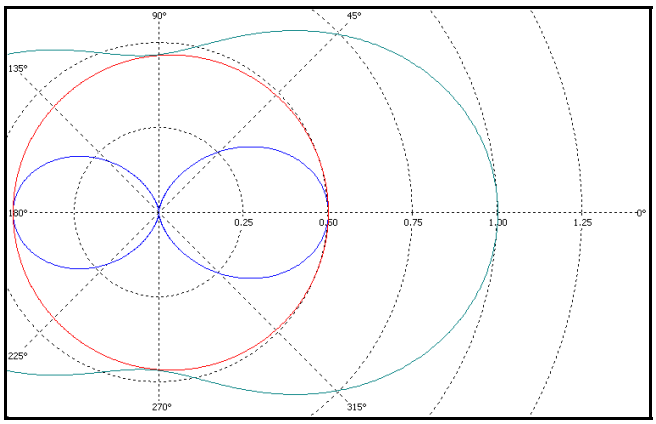

Figure 5: Normalized scattered intensity; radius a=0.25 mm, 59 GHz, 20°C

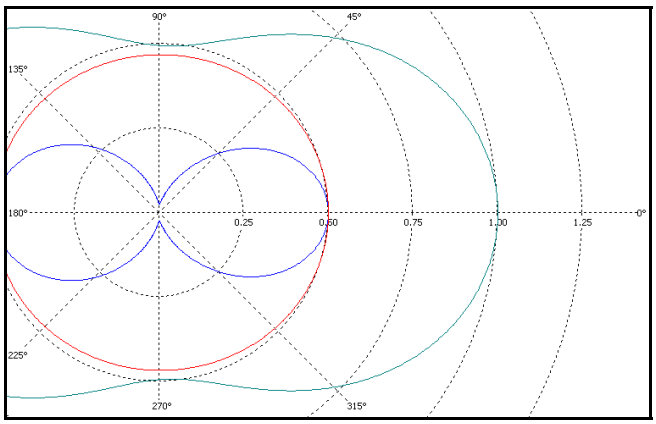

Figure 6: Normalized scattered intensity; radius a=0.5 mm, 59 GHz, 20°C

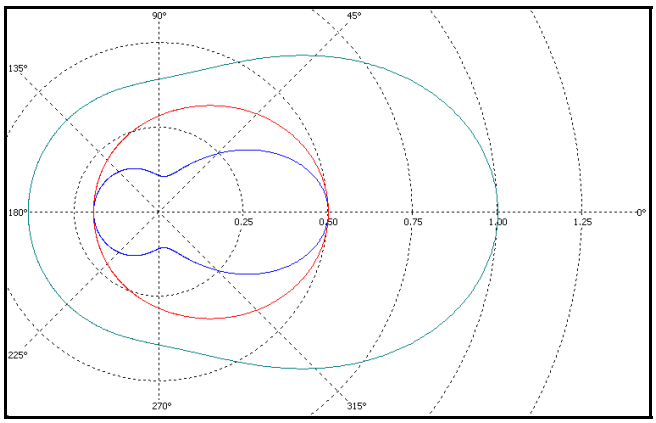

Figure 7: Normalized scattered intensity; radius a=1.0 mm, 59 GHz, 20°C

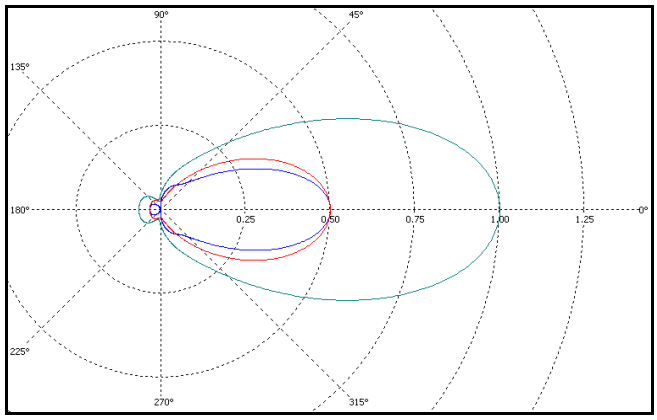

Figure 8: Normalized scattered intensity; radius a=2.0 mm, 59 GHz, 20°C

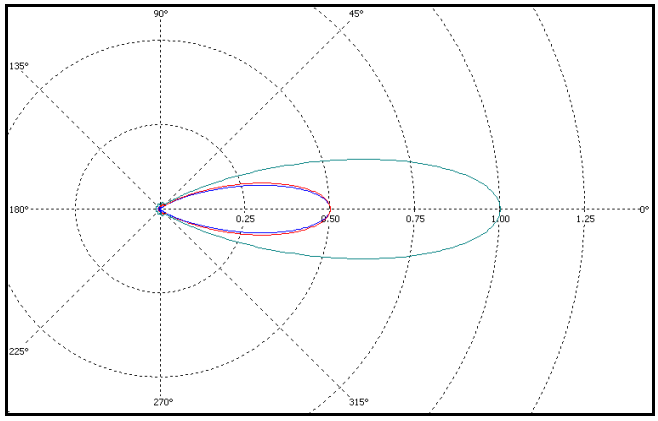

Figure 9: Normalized scattered intensity; radius a=4.0 mm, 59 GHz, 20°C

IV. Analysis of Link Measurements

As part of an Ofcom study carried out in 2003/2004, rain scattering measurements at 60GHz were made by QinetiQ [10]. For the measurements, an experimental propagation link was established using a wideband channel-sounder (MEDAV RUSK). The transmitter antenna was fed with an RF power of +5.1 dBm. The transmitter and receiver antennas were lens horn antennas with a gain of 34.5 dBi. The half-power beamwidth of the antennas was 3˚ which is comparable with that of typical commercial equipment. The receiver noise bandwidth was 120 MHz. The antennas were located in two buildings at QinetiQ's Great Malvern site, with a line-of-sight distance of 75 m.

Using experimental equipment specification described above the scattering model described in Section II was used to investigate the level of bistatic coupling. The received power as a function of scattering angle was determined, taking account of the excess oxygen attenuation (using the model of [11]) and free-space path loss. Figure 10 shows an example of this calculation for Marshall-Palmer rainfall at a rate of 20 mm h^{-1}. This rainfall rate is exceeded for approximately only 0.01% of the time for the majority of Europe.

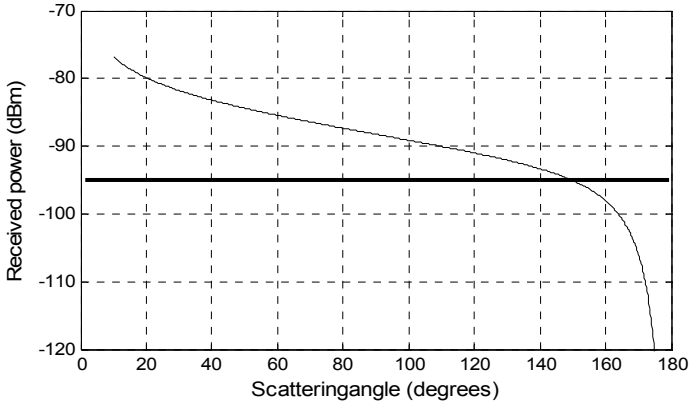

Figure 10: Received signal level as a function of scattering angle for the scenarios described above at 20 mm h^{-1} (thin line). Forward scattering corresponds to 0˚, backscattering corresponds to 180˚. Receiver noise floor corresponds to approximately -95 dBm (thick line).

At this relatively high rainfall rate it can be seen that there is strong forward scattering and relatively weak backscattering. In addition to and in spite of the additional attenuation due to oxygen (albeit over a very small link in this instance) bistatic coupling causes a ~10 dB enhancement in the noise for scattering angles up to 45˚. Orthogonal (crossing links) demonstrate around ~7 dB enhancement.

For a bistatic scattering angle of 45˚, Fig. 11 shows a typical result of the measured received power, together with the calculated power (derived from the theoretical model) and the associated rainfall rate. It can be seen that there is good agreement between the calculated power and the measured data. Note that even the light rainfall rates of this event, peaking at around 8 mm h^{-1} caused significant bistatic coupling of the order of 2-3 dB in the model case and around 3-4 dB in the experimental case.

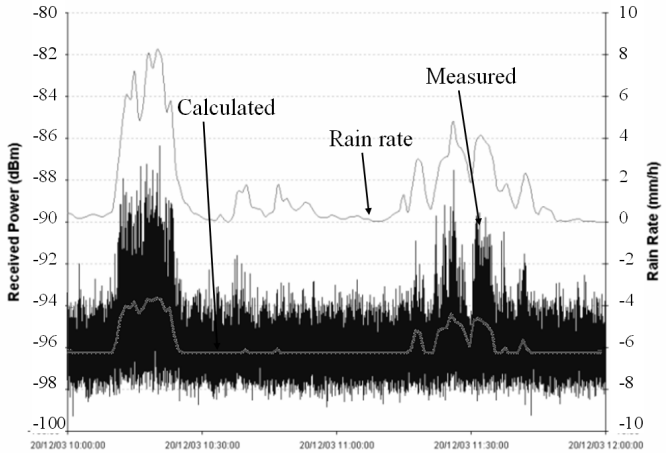

Figure 11: Comparison between measured and modelled bistatic received signal power (lefthand axis) 10:00-12:00 UTC 20/12/2003. Rainfall rate as measured by a Thies Clima laser distrometer is also shown (righthand axis)

V. Conclusions

This paper has shown that, in the context of the widespread deployment of 60 GHz links, coupling between adjacent links caused by bistatic scattering can be evident even for light rainfall. This effect has been shown experimentally and through modelling and occurs in spite of the high oxygen attenuation. Although best agreement between model and measurements was observed using a Marshall-Palmer raindrop size distribution, it should be noted that in many cases the Marshall-Palmer distribution can substantially overestimate the number of smaller raindrops and therefore overestimate the scattered power. Further experimental study is required to fully investigate the possible link scenarios that are most susceptible to bistatic coupling.

Acknowledgments

We thank Ofcom and Dr A. Shukla of QinetiQ for making available the experimental data used in this study which was originally collected under Ofcom contract AY4497.

References

[1] A. Ishimaru, *Wave Propagation and Scattering in Random Media*, IEEE Press and Oxford University Press, 1997.

[2] R. K. Crane, "Bistatic Scatter from Rain," *IEEE Trans. Antennas Propagation*, vol. 22, pp 312–320, March 1974.

[3] M. O. Ajewole and T. Oguchi, "Effects of multiple scattering on communication at millimetre and centimetre wavelength in tropical rainfall conditions", *Electronics Letters*, Vol 37, No2., pp121-123, January 2001.

[4] T. Oguchi, "Effects of incoherent scattering on microwave and millimetre wave communications through rain", *Electronics Letters*, 18th January 1991, Vol 27, No9., pp759-761

[5] C. Gloaquen and J. Lavergnat, "94 GHz Bistatic Scattering in Rain," *IEEE Trans. Antennas Propagation*, vol. 44 pp 1247–1258, Sept. 1996.

[6] C. J. Gibbins and S. Cirstea, "Development of a numerical integration rain scatter method for recommendation ITU-R P452", Final report on project AY4209, Radiocommunications Agency, 2003.

[7] ITU-R P.452-13, "Prediction procedure for the evaluation of microwave interference between stations on the surface of the Earth at frequencies above about 0.7GHz", ITU-R Recommendations, 2007

[8] H. T. van der Zanden, R. J. Watson and M. H. A. J. Herben, "Rain-induced bistatic scattering at 60 GHz", EURASIP Journal on Wireless Communications and Networking, Vol. 2007, doi:10.1155/2007/53203.

[9] M. Kerker, *The Scattering of Light – and other electromagnetic radiation.* London: Academic Press, Inc., 1969.

[10] R. M. Swindell, D. J. Fraser and R. J. Watson, "Improving Spectrum Utilization at 58-66 GHz through an Accurate Assessment of Rain Scatter Interference" Final report on AY4487, Ofcom, 2004.

[11] H. J. Liebe, "MPM – An Atmospheric Millimeter-Wave Propagation Model*" International Journal of Infrared and Millimeter Waves*, Vol.10, No. 6, 1985.